NUMERICAL ANALYSIS OF WELLS TURBINE FOR WAVE POWER CONVERSION

Z. Čarija[1*] – L. Kranjčević[1] –V. Banić[2] – M. Čavrak[1]

[1]Department of Fluid Mechanics and Computational Engineering, Faculty of Engineering, University of Rijeka, Vukovarska 58, Rijeka
[2]Faculty of Engineering, University of Rijeka, Vukovarska 58, Rijeka

ARTICLE INFO

***Article history*:**
Received 26.04.2012.
Received in revised form 17.07.2012.
Accepted 17.07.2012.

Keywords:
Wells turbine
Oscillating water column plant
Sea wave energy
CFD simulation

Abstract:

Sea wave energy is one of the high potential renewable energy sources. The Wells turbine as the main part of Oscillating Water Column energy plant is analyzed in this paper. The Wells turbine uses air flow produced by the pressure change inside the oscillating water column. Efficient energy transformation is achieved with the use of self-rectifying Wells air turbine. Since the tangential force of the rotor acts only in one direction, even though airflow is oscillating, turbine rotates always in the same direction. Series of numerical simulations are performed using software package FLUENT for a wide span of the non-dimensional flow rate coefficient ϕ and employing three different turbulent models. Structured numerical mesh and the application of axisymmetric periodical boundary conditions raised the accuracy of the numerical model while reducing computational load three times compared to the model with the fully meshed domain. Finally, the operation of the OWC plant consisting of the air chamber and the turbine was simulated for maritime conditions in the Adriatic sea giving satisfactory energy output by taking into consideration a compact dimension of the whole plant.

1 Introduction

The rising cost of fossil fuels and greater awareness about their influence on the environment shifts the public and engineering interest towards the renewable energy sources. One of high potential renewable energy sources is certainly sea wave energy. Sea waves are formed by wind blowing over vast areas of the seas and they have substantially greater energetic potential than wind or solar energy. One of the most promising devices for sea wave energy harnessing is based on the Oscillating Water Column (OWC) principle. It uses the air flow produced by the pressure change inside the

* Corresponding author. Tel.: +385 51 651 554; fax: +385 51 651 416
E-mail address: zoran.carija@riteh.hr

oscillating water column. Efficient energy transformation is achieved with the use of self-rectifying air turbines. There are currently three different types of self-rectifying air turbines: Wells turbine, Impulse turbine and Dennis-Auld turbine. The Wells turbine is the oldest concept of the self-rectifying air type turbine. It was introduced in 1976 by Prof. A. A. Wells from the Queen's University in Belfast. Multiple authors have conducted some research into different aerodynamic blade profiles of the Wells turbine [1-5]. Thakker and Abduladi [1], compared the experimental results of four different aerodynamic blade profiles (NACA0015, NACA0020, CA9 and HSIM 15-262123-1576). They concluded that CA9 and NACA 0020 with rotor solidity σ=0.64 are the most suitable blade profiles for the Wells turbine due to high efficiency achieved in the widest operating range of the flow rate coefficient ϕ compared to other analyzed profiles. Besides experimental testing, many authors have used numerical fluid flow simulations in order to determine performance curves of Wells turbines with different blade shapes and solidity. Fluid flow simulations were carried out for the following aerodynamic blade profiles: CA9 [2], NACA 0015 [3], NACA 0020 [4] and NACA 0021 [5]. Our intention is to compare numerically achieved performance characteristics of the Wells turbine with a particular blade profile to the available experimental data. The paper by Dhanasekaran and Govardhan [5] providing experimental data for the Wells turbine with constant chord NACA 0021 aerodynamic blade profile is chosen. Numerical analysis is performed using commercial fluid flow solver FLUENT®. Three different *RANS* turbulent models (*k*-ε realizable, RNG *k*-ε and SST *k*-ω) are used and their results are compared to the experimental data.

2 The Wells turbine description

The principle of the Oscillating Water Column (OWC) plant is shown in the Fig. 1.
The main elements of the plant are the air chamber and the Wells turbine with the electric generator. The Wells turbine consists of the rotor blades with symmetrical airfoil cross section set radially around the central hub, Fig. 2.

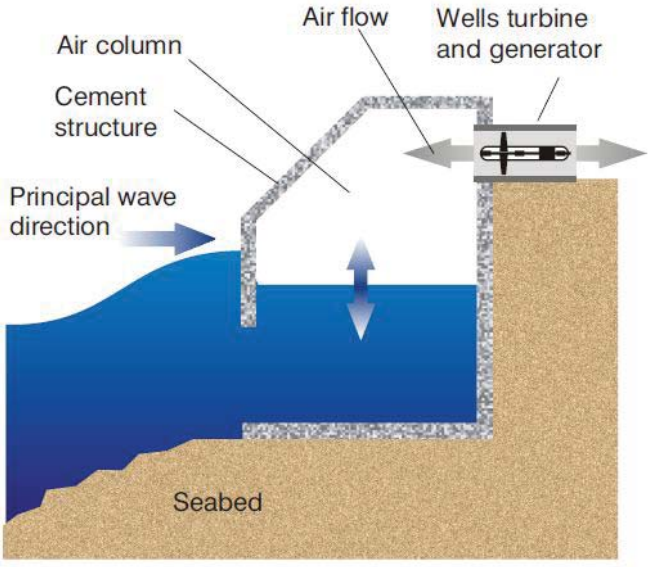

Figure 1. Concept of the Oscillating Water Column energy plant

Turbine blades are positioned symmetrically with respect to the plane normal to the central axis. This type of blade positioning makes the turbine non-sensitive to the incoming flow direction. The tangential force of the rotor acts only in one direction even though airflow oscillates. Consequently, the turbine rotates always in the same direction and runs the electrical generator regardless of the airflow direction. The operation principle of the Wells turbine has been shown in Fig. 2. Fluid flow at the angle of incidence, α will generate lift force L normal to the free stream and a drag force D in the free stream direction. These forces can be resolved into a tangential component F_θ, which creates torque around the axis of the turbine and an axial component F_χ which causes thrust along the axis of the turbine [6]. Thus, for a rotating turbine in oscillating flow, the angle of incidence varies from positive to negative value with the mean value of 0. Considering the aerofoil being symmetrical, tangential force F_θ acts in the same direction independently of positive or negative values of the angle α. In this way, unidirectional torque from an oscillating flow is created [6]. The turbine performance can be expressed in terms of three non-dimensional coefficients - pressure Ψ, torque Π, and efficiency η:

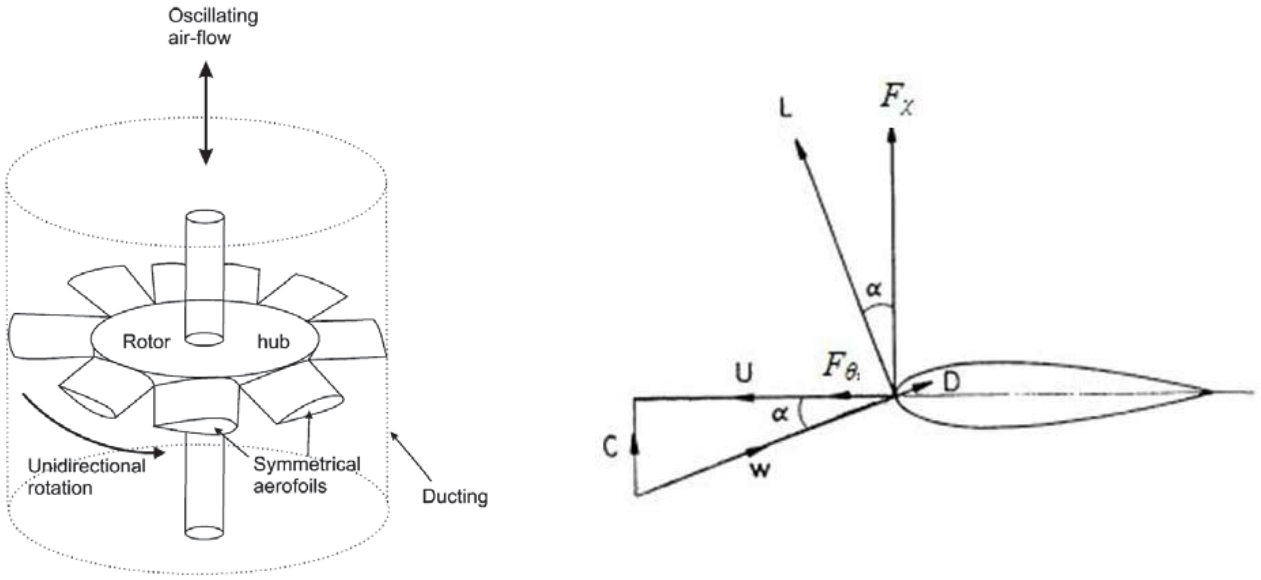

Figure 2. Wells turbine operation principle. Velocity vectors: C – absolute velocity; U – angular velocity; W – relative velocity

$$\Psi = \frac{\Delta p}{\rho_a \omega^2 r_t^2} \tag{1}$$

$$\Pi = \frac{T}{\rho_a \omega^2 r_t^5} \tag{2}$$

$$\eta = \frac{T\omega}{\Delta p Q} \tag{3}$$

where Δp is the pressure drop across the turbine, ρ_a is the density of air, ω is the speed of the turbine rotation, r_t is the turbine rotor radius, Q is the volume flow rate through the turbine, and T is the turbine torque. For any particular turbine, these parameters depend on the flow rate coefficient ϕ (the ratio of axial air velocity v and rotor tip speed ωr_t). The flow rate coefficient reads:

$$\phi = \frac{Q}{\omega r_t^3 \pi} = \frac{v}{\omega r_t}. \tag{4}$$

Compressibility effect is neglected because of the low Mach number flow.

3 Numerical analysis

Geometry of the numerical model is made according to the experimental model presented in [5]. Tip clearance has been omitted in the numerical model in order to simplify the numerical mesh generation. This modification influences the final result minimally for the low tip clearance of 1% (tip gap in percent of chord value) as in our case [3]. Geometry of the model supply pipe consists of the initial 200 mm long and 250 mm diameter pipe connected with the 25 mm long cone to the main part of the 265 mm diameter supply pipe, Fig. 3. 3D assembly model of Wells turbine is made using software package CATIA V5R18®, Fig. 3. The turbine presents following characteristics:

- number of blades N = 4;
- constant chord length c = 0,1 m;
- tip radius R_{tip}= 0,1325 m;
- hub-to-tip ratio h = 0,619;
- blade solidity σ = 0,59;
- NACA 0021 aerodynamic profile;
- Constant angular velocity ω = 4500 rpm;

When taking into account the axisymmetric geometry of the turbine, it is not necessary to mesh the whole geometry of the turbine but only one quarter of an overall domain, Fig. 3. Periodical boundary conditions are imposed on the neighboring surfaces of the turbine. Geometry of the model is divided into three parts (domains) in order to simplify the meshing process (inlet part with the top of the hub, middle part with the turbine blade, and exit part). Final turbine model assembly is shown in Fig. 3. GAMBIT 2.4.6 was used for meshing the model and numerical simulation was performed using FLUENT 6.3.26. Inlet part of the domain was meshed with 114186 elements of the numerical mesh.

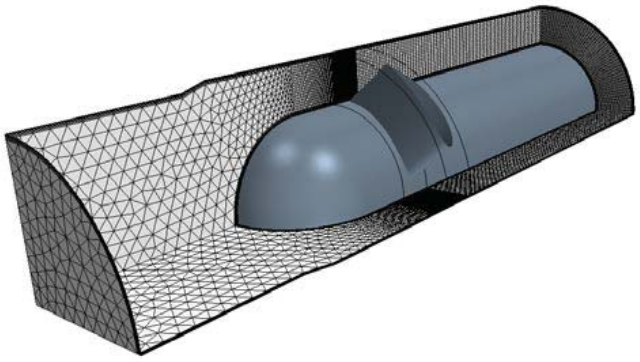

Figure 3. Geometry and numerical mesh of the 1/4 Wells turbine model

Elements of the mesh are gradually reduced in size towards the middle part of the domain. The middle part of the domain was meshed with 220500 hexahedral elements from the numerical mesh while the exit part of the domain was meshed with 90000 hexahedral elements. The six cell boundary layer is placed on domain walls with the size of the first element that ensures Y+>30 value in all investigated cases. The total number of cells is 424686. Periodical boundary conditions are imposed on the surfaces adjacent to the non-modeled parts of geometry. The velocity inlet boundary condition is set at the domain entrance located 4 blade chord lengths from the runner central section while the free outflow boundary condition is set at the 8 blade chord length distance. Turbulence quantities at the inlet are calculated using turbulence intensity and the hydraulic diameter. The hydraulic diameter equals the supply pipe diameter while turbulence intensity is estimated using an empirical correlation for pipe flows, dependent on the Reynolds number [7]. The model accuracy is preserved with a simultaneous increase in cell density around the turbine blade. Numerical cells in the middle part of the domain rotate together with the blades of the turbine with the constant angular speed $\omega = 4500$ rpm. No-slip boundary conditions are imposed on the domain walls. Separate domains are connected with non-conformal grid interfaces. Implicit Navier-Stokes equations pressure based solver is used together with the SIMPLEC method for linking pressure and velocity fields and using second order discretization for convective fluxes. Three different turbulent models are used: RNG k-ε model, Realizable k-ε model, and SST k-ω turbulent model. RNG k-ε model and Realizable k-ε model non-equilibrium wall functions are used for the near-wall modeling, while SST k-ω turbulent model uses specific wall treatment. Non-equilibrium wall functions proved to be more suitable than standard wall functions due to the flow separation occurring in the Wells turbine. Non-equilibrium wall functions gave more accurate results during validation simulations. Two additional control planes have been created inside the domain in order to calculate integral quantities. The first control plane precedes the turbine and is set 33 mm in front of the runner inlet while the second one is set 80 mm behind the runner outlet.

4 Simulation results and application

Numerical simulations covered eight different cases of constant flow. Performance characteristics of the turbine are described using three dimensionless coefficients: pressure coefficient Ψ (1), torque coefficient Π (2) and efficiency η (3). Dependence of these coefficients on the flow rate coefficient ϕ is shown in charts given in Figs 4-6.

Structured numerical mesh and the application of axisymmetric periodical boundary conditions raised the accuracy of the numerical model while reducing computational load three times in comparison to the model with fully meshed domain [5]. Fig. 4 shows that calculated efficiency is in good agreement with the experimental data almost through the whole range of the analyzed flow rate coefficient span. Additional numerical accuracy improvements can be achieved using enhanced wall functions and appropriate increment in mesh density around the turbine blades. Fig. 4 shows that the best agreement with the experiment is achieved with the Realizable k – ε turbulent model. The best efficiency is somewhere around 60% for the applied k-ε turbulent model and 55% for the SST k – ω turbulent model at the non-dimensional flow coefficient value ϕ=0,155. The largest deviation from the experimental data is most likely observed at low flow rates because of the unfavorable position of the inlet grid interface with respect to the direction of the incoming relative velocity. Figs 5 and 6 show that pressure and torque coefficients increase when the flow rate coefficient ϕ increases. Pressure and stall torque coefficients occur (ϕ=0.21) at the highest analyzed fluid flow rates when the fluid flow starts to separate from the suction side of the blade surface.

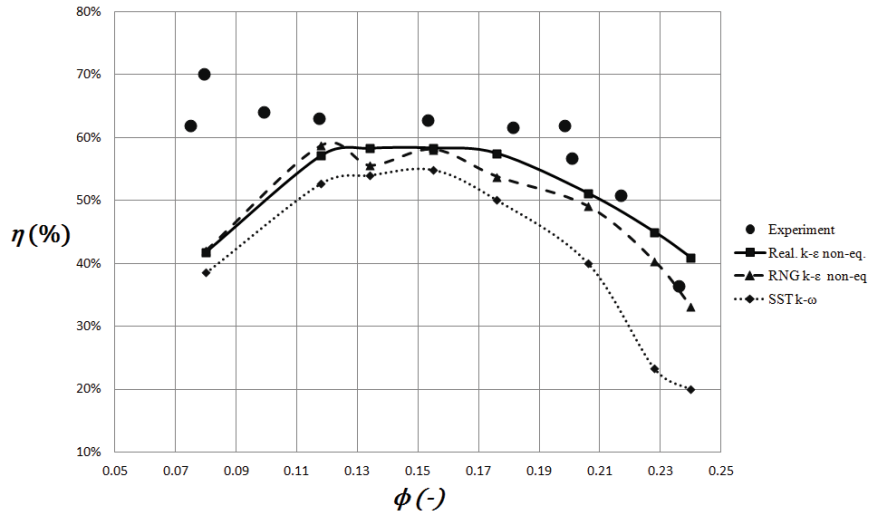

Figure 4. The efficiency of the Wells turbine, η

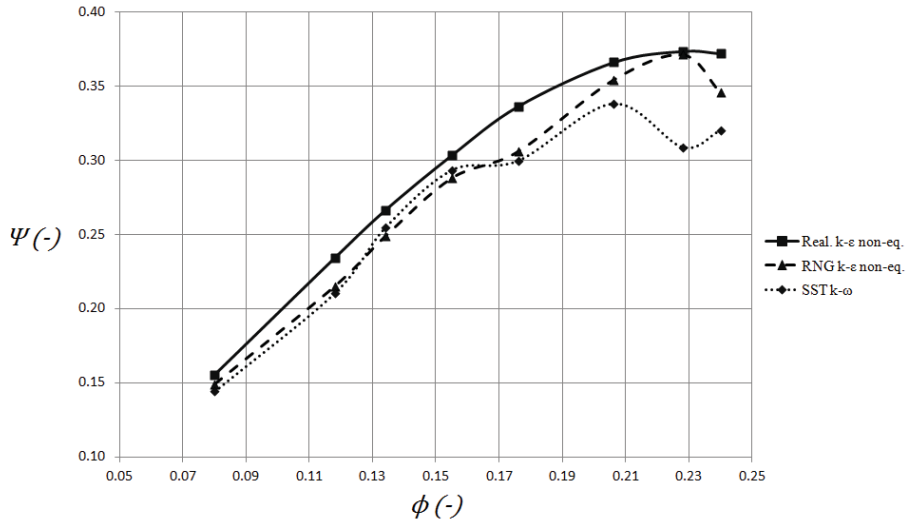

Figure 5. Pressure coefficient, Ψ

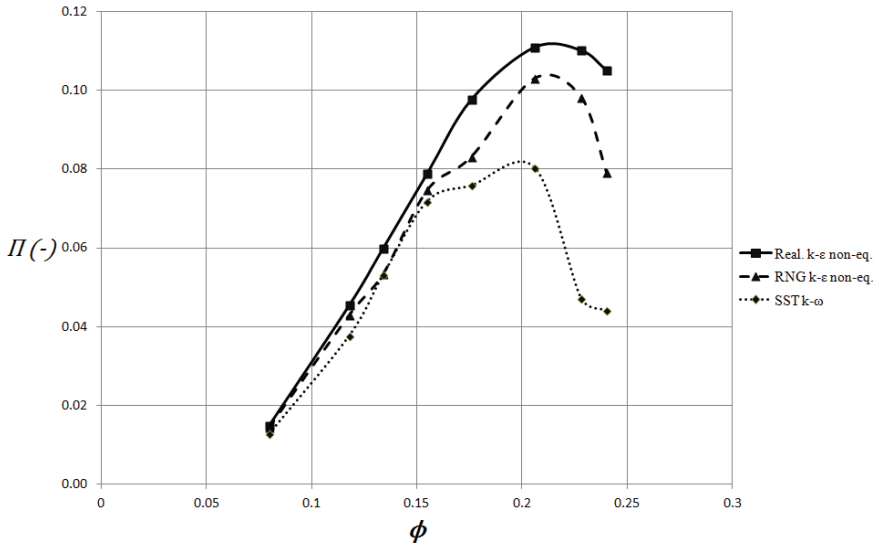

Figure 6. Torque coefficient

Further increasing of the flow rate coefficient causes a rapid growth of the separation zone on the blade suction side, reducing the values of the pressure and torque coefficient even more ($\phi>0.23$). As a consequence of the fluid flow separation from the runner blade surfaces, efficiency drops in the incipient and deep stall flow rate range. To confirm the potential for the practical use of the modeled turbine, performance curves obtained from the numerical simulations are used for its application under real maritime conditions. Therefore, the operation of the modeled OWC plant was simulated for maritime conditions in the Adriatic sea using the average sea wave height of $h=1,3$ m and wave period of $T=5,4$ s. These data are taken as the average coastal condition wave data in the Adriatic given in [8] and [9]. Sinusoidal sea wave height change h determines the turbine flow rate coefficient ϕ necessary for the determination of torque (Π) and pressure (Ψ) coefficients using ϕ-Ψ and ϕ-Π relations (Fig. 5 and 6). The torque (calculated from the torque coefficient Π) is used to calculate power production ($P = T\omega$). Therefore, operation of one OWC plant would produce 1850 kWh of energy per year for the assumed average sea regime data. Considering the very compact dimensions of the simulated OWC plant (the air chamber with 0,55 m^2 cross section area and 265 mm diameter turbine), energy output can be increased by creating an array of small plants. Installation of that kind could be used as the energy source for various remote maritime facilities e.g. offshore installations or isolated island households etc.

5 Conclusion

In this paper operational characteristics of the Wells turbine with NACA 0021 aerodynamic blade profile are analyzed with different coefficients of air inflow. Numerical simulations are performed employing software package FLUENT using three different turbulent models RNG $k-\varepsilon$ turbulent model, Realizable $k-\varepsilon$ turbulent model and SST k-ω turbulent model. The best results are achieved using Realizable $k-\varepsilon$ turbulent model. Highest calculated efficiency of the Wells turbine is calculated to be around 60% for non-dimensional flow coefficient ϕ=0,155. Structured numerical mesh in the turbine blades area and the use of periodical domain boundaries contributed to the greater accuracy of the numerical simulations in comparison with the previous numerical analysis of the same turbine [5]. Finally, the operation of the OWC plant consisting of the air chamber and turbine was simulated under maritime conditions in the Adriatic sea giving satisfactory energy output by considering compact dimension of the whole plant. Additional research should be concentrated on the analysis of turbine blade tip clearance, optimal blade shape and the shape of air chamber geometry for operating conditions.

References

[1] Thakker, A., Abdulhadi, R.: *The performance of Wells turbine under bi-directional airflow*, Renewable Energy, 33 (2008), 11, 2467–2474.

[2] Thakker, A., Frawley, P. i Sheik Bajeet, E.: *Numerical Analysis of Wells Turbine Performance Using a 3D Navier-Stokes Explicit Solver.* Proceedings of the Eleventh International Offshore and Polar Engineering Conference. Stavanger, Norway, 2001, 604-608.

[3] Torresi, M., Camporeale, S.M., Strippoli, P.D., Pascazio, G.: *Accurate numerical simulation of a high solidity Wells turbine,* Renewable Energy, 33 (2008), 4, 735-747.

[4] Kinoue, Y., Kim, T.H., Setoguchi, T., Mohammad, M., Kaneko, K., Inoue, M.: *Hysteretic characteristics of monoplane and biplane Wells turbine for wave power conversion*. Energy Conversion and Management, 45 (2004), 9-10, 1617–1629.

[5] Dhanasekaran, T.S., Govardhan, M.: *Computational analysis of performance and flow investigation on wells turbine for wave energy conversion,* Renewable Energy, 30 (2005), 14, 2129–2147.

[6] Folley, M., Curran, R., Whittaker, T.: *Comparison of LIMPET contra-rotating wells turbine with theoretical and model test predictions*, Ocean Engineering, 33 (2006), 8-9, 1056-1069.

[7] Fluent 6.3 Documentation, User's Manual, Fluent Inc., 2006.

[8] Zorović, D., Mohović, R, Mohović, Đ., *Toward Determining the Length of the Wind Waves of the Adriatic Sea*, Naše more, 50(2003) 3-4.

[9] *Pomorska enciklopedija*, Leksikografski zavod Miroslav Krleža, Zagreb, 1976., sv. 3, str. 210 (*Jadransko more*).